RSC Advances

PAPER

View Article Online
View Journal | View Issue

Cite this: *RSC Adv.*, 2019, **9**, 2395

Facile and green preparation of hemicellulose-based film with elevated hydrophobicity *via* cross-linking with citric acid

Hui Shao, Hui Sun,* Biao Yang, Huijuan Zhang and Yu Hu

Hemicellulose has shown great potential in food packaging due to its excellent biodegradability and low oxygen permeability. However, its strong hydrophilicity leads to poor moisture resistance and hinders its wide application. To address this issue, herein a ternary carboxylic acid, citric acid (CA), was incorporated into hemicellulose as esterifying agent to form a crosslinking structure *via* the esterification reaction. The CA-modified hemicellulose films showed an increased contact angle of 87.5° (*vs.* 40.5° for unmodified film), demonstrating that the hydrophobicity of hemicellulose had been improved significantly. In addition, the esterification/cross-linking modification enhanced oxygen barrier performance with oxygen permeability decreasing from 1053 (cm^3 μm) (m^2 d kPa)$^{-1}$ to 1.8 (cm^3 μm) (m^2 d kPa)$^{-1}$. Moreover, the tensile strength rose to a peak value and then fell back at higher CA content. Effect of CA addition on elongation at break exhibited an opposite trend. The modified hemicellulose films with 20% CA addition possessed the highest tensile strength and the lowest elongation at break. Morphology observation with scanning electron microscopy indicated that at CA content exceeding 20%, the modified films were dense with a smooth surface, illustrating the improvement of phase compatibility. A possible mechanism for esterification/cross-linking was proposed to elucidate the connection between CA addition and film performances.

Received 3rd December 2018
Accepted 8th January 2019

DOI: 10.1039/c8ra09937e

rsc.li/rsc-advances

Introduction

With the deterioration of the ecological environment, it is necessary to replace petroleum-based materials with eco-friendly lignocellulosic biomass consisting of cellulose, hemicellulose and lignin to produce chemicals and materials.[1–3] Among the three main components of biomass, hemicellulose, the most abundant biomass resource second only to cellulose, has attracted increasing research attention. Hemicellulose shows such characteristics as renewability, biodegradability and excellent oxygen barrier property and thus is promising in potential application fields of agriculture, food packaging, biomedicine, and so forth.[4,5] However, the strong hydrophilicity makes hemicellulose films fragile under humid conditions, resulting in poor mechanical properties due to the phase separation when blending with hydrophobic polymers. These drawbacks limit the application of hemicellulose in high-value-added industries.[6] Some efforts have been devoted to increasing the hydrophobicity of hemicellulose *via* chemical modification, *i.e.* esterification,[7,8] acetylation,[9–11] etherification,[12–14] fluorination[15,16] and cross-linking.[17–19]

Esterification of hemicellulose refers to the reaction between the hydroxyl groups on the molecular chains and carboxylic acids or acid derivatives (anhydride, acyl chloride).[6] The hydrophobicity of hemicellulose and its compatibility with thermoplastic polymers can be improved *via* hydrophobic conversion of the hydrophilic hydroxyl groups. Esterified hemicellulose can even be dissolved in organic solvents eventually.[7] Differing from traditional esterifying agents like acetic acid[10] and butyl chloride,[20] CA is an inexpensive and safe food additive, which can react with hemicellulose under mild conditions and form a cross-linking structure in the meantime. Wang and co-workers performed the esterification of poly(vinyl alcohol) (PVA)/xylan composite films by using CA to enhance the mechanical properties.[21] The reaction mechanism and the effect of CA contents on the hydrophobicity and oxygen permeability have not been investigated yet.

In the investigation mentioned above and many other literatures on hemicelluloses, PVA[22] or other polymer *i.e.* carboxyl methyl cellulose[23] or chitosan[24] is often added as co-matrix to improve the film formability.[25] To the same end, plasticizers such as glycerol, sorbitol, xylitol are also added to obtain continuous and self-supporting hemicellulose films.[26] In this work, hemicellulose was isolated from poplar powder through the procedure of alkaline hydrolysis followed by alcohol precipitation. Sorbitol and PVA were added to improve the film-forming ability of hemicellulose. Then, through an esterification/cross-linking reaction by incorporation of citric acid, a series of hydrophobically modified hemicellulose films were obtained by solvent

School of Materials Science and Mechanical Engineering, Beijing Technology and Business University, Beijing 100048, P. R. China. E-mail: sunhui@th.btbu.edu.cn

casting method. The properties (thermal, mechanical, barrier, wettability) of the film were investigated and modified by varying the CA content. A mechanism is proposed for the esterification/cross-linking reaction to elucidate the CA content dependence of film performance. This research is directed to better understanding of the modification and thereby for a better application of the renewable film with excellent barrier performance as alternative packaging material.

Experimental

Materials and reagents

Poplar wood powder with particle size between 0.2–0.8 mm was collected from five-year poplar with hemicellulose content of 30.5% in Hebei province and the main components of hemicellulose were 4-*O*-methyl glucuronic acid xylose. Sodium hydroxide, sodium chlorite, hydrochloric acid, sorbitol and CA (of analytical purity, Sinopharm Chemical Reagent Co., Ltd.), glacial acetic acid (Beijing Chemical Plant), ethanol (95%, w/v, Tianjin Oko Chemical Reagent Co., Ltd.) and PVA (with degree of polymerization of 1700 and alcoholysis degree 99%, China Petrochemical Co., Ltd) were all used as received.

Extraction of poplar hemicellulose

Hemicellulose was isolated from poplar powder through an alkaline hydrolysis followed by alcohol precipitation approach (Fig. 1).[27] Dried poplar powder was Soxhlet extracted for 6 h using toluene/ethanol (2 : 1, volume ratio) and then dried for 12 h at 60 °C. The obtained defatted sample was re-extracted with 0.6% (w/v) sodium chlorite solution for 1 h at 75 °C. The solid–liquid ratio was 1 : 20 (w/v) and the pH was adjusted to 4.0 with glacial acetic acid. After being rinsed and dried, the filter residue was put into 9.5% (w/v) NaOH solution for 4.2 h at 78 °C. The solid–liquid ratio was also 1 : 20 (w/v). After the pH was adjusted to 5.5 with muriatic acid, the filtrate (containing hemicellulose) was precipitated with 95% (w/v) ethanol (1 : 3 v/v). The mixture was left to stand for 12 h before polar hemicellulose was obtained by centrifugation followed by drying the filter residue.

The weight average molecular weight (M_w) of obtained hemicellulose was about 23 380 g mol^{-1} as determined by gel chromatography and 4-*O*-methyl glucuronic acid xylan was the main component as revealed by ion chromatography analysis.[27,28]

Table 1 Designation of hemicellulose films with CA of different proportions

Sample	Hemicellulose (g)	PVA (g)	Sorbitol (g)	CA (g)
Blank	0.90	0.30	0.30	0.00
H_1	0.90	0.30	0.30	0.15
H_2	0.90	0.30	0.30	0.30
H_3	0.90	0.30	0.30	0.45
H_4	0.90	0.30	0.30	0.60
H_5	0.90	0.30	0.30	0.75

Preparation of hydrophobic hemicellulose films

The main composition of each film is as follows: 60% poplar hemicellulose (w/w), 20% PVA (w/w), and 20% sorbitol (w/w). The total mass of the above three components was 1.5 g. The controlled film without any additives was designed as blank. Films with CA fraction of 10%, 20%, 30%, 40% and 50% were denoted as H_1, H_2, H_3, H_4 and H_5 respectively (Table 1).

PVA was pre-dissolved in water at 95 °C in a beaker. Then hemicellulose, sorbitol and CA of different amounts were added and the mixture was stirred for 4 h at 75 °C. Well-proportioned and stable solutions were treated in an oven at 110 °C for 2.5 h followed by ultrasonic treatment for 10 min (59 kHz). The solutions were cast into polystyrene culture dishes (130 mm × 130 mm) and vacuum defoamed for 15 min. Water was evaporated in an oven at 50 °C and the dried films were left to stand overnight at room temperature prior to all measurements.

Analytical methods

Infrared spectrum analysis (FT-IR). The chemical functional groups of hemicellulose were analyzed on a Fourier infrared spectroscopy analyzer (iN10 MAX, Thermo Scientific Co., Ltd.). The spectra were obtained at the resolution of 4 cm^{-1} with 32 scans in the range from 4000 to 450 cm^{-1}.

Thermogravimetric analysis (TGA). Thermal stability of the films was carried out on thermogravimetric analyzer (Q50, TA Instruments). The test temperature ranged from 40 °C to 600 °C with the nitrogen flow rate maintained at 100 mL min^{-1} and the heating rate of 20 °C min^{-1}.

Tensile test. According to China national standard GB/T1040.2-2006, the film sample was cut into a rectangular specimen of 10 mm × 80 mm. The tensile test of the films was

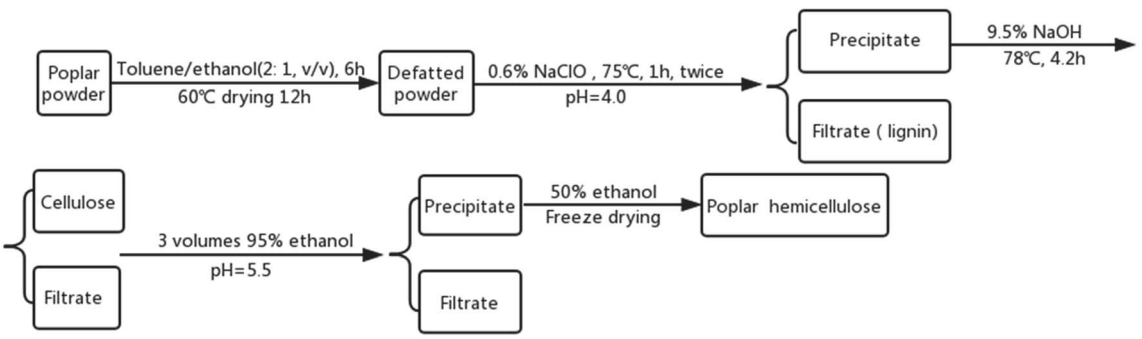

Fig. 1 Flow chart for alkaline extraction of hemicellulose.

performed with a universal material testing machine (CMT6104, MTS Systems Co. Ltd., China). The initial distance between the grips and the cross-head speed was kept constant at 80 mm and 5.0 mm min^{-1}, respectively. Tensile strength and elongation at break values of the films were averaged over five specimens.

Scanning electron microscopy analysis (SEM). The surface morphologies of the films were observed using a scanning electron microscope (Quanta FEG 250, FEI). The film was cut into small pieces, and sputter-coated with a thin layer of gold prior to the examination in order to make the films conductive. The test was operated in high-vacuum mode with an acceleration voltage of 10 kV.

Oxygen permeability (OP) measurement. The oxygen barrier properties of the composite films were assessed on a circle sample surface (10 cm in diameter) by use of a VAC-V2 permeability analyzer (OX-TRAN 2/21, MOCON). The measurements were conducted at 23 °C under 50% relative humidity (RH) condition according to standard method described in China national standard GB/T 1038-2000. The OP is given in unit of [(cm^3 μm) (m^2 d kPa)$^{-1}$]. Each result was averaged over three specimens.

Contact angle test. Contact angles were measured on a goniometer equipped with a measuring video system (OCA35, DataPhysics Instruments GmbH). Water droplet of 2 μL was carefully injected onto the film surface. Then an image of the droplet was captured from which a contact angle measurement can be obtained. Five different locations on each sample were tested and the mean was taken as the static contact angle.[29]

Results and discussion

Mono-esterification reaction can improve the hydrophobicity of hemicellulose to some extent. However, the increase in molecular chain flexibility results in the decreasing mechanical properties. In this investigation, an inexpensive, non-toxic ternary carboxylic acid CA, was selected as esterification agent to construct cross-linked structure (Fig. 2) at high temperature with the aim of enhancing the mechanical strength and moisture resistance of hemicellulose films.

Surface hydrophobicity analysis of modified hemicellulose films

For evaluating the hydrophobicity of modified hemicellulose films, the contact angle of the film was measured by the sessile drop method. Five different locations on each sample were tested and the mean was taken as the static contact angle. Vogler[30] defined hydrophobic surfaces (contact angle higher than 65°) and hydrophilic surfaces (contact angle less than 65°) on the basis of the observation that there are two distinct kinds of water structure and reactivity, which was revealed by using a surface force apparatus and ancillary techniques. The test results were shown in Fig. 3.

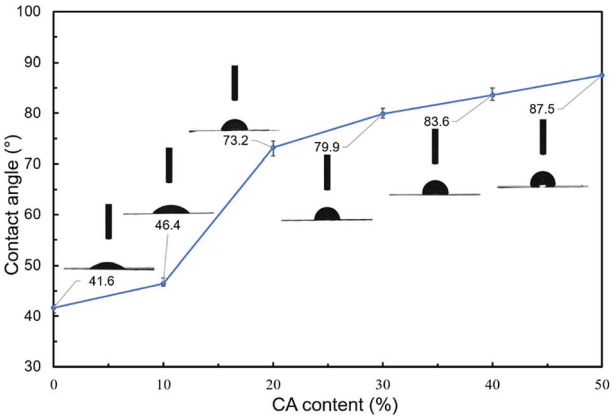

Fig. 3 Contact angle results of modified hemicellulose films.

The contact angles were measured to be 41.6°, 46.4°, 73.2°, 79.9°, 83.6° and 87.5° for blank, H_1, H_2, H_3, H_4 and H_5 respectively. As is shown, with the increase of CA content, the contact angle of poplar hemicellulose film gradually increased, indicating that the wettability gradually became worse, namely the hydrophobic performance of the surface was enhanced. Among them, the difference gap of contact angle between H_1 and H_2 films was up to 26.8°, which meant the hydrophilic surfaces turned hydrophobic, indicating the remarkable effect of hydrophobic modification *via* adding 20% CA. When CA content is further increased, the increase in contact angle becomes less marked, showing that further addition of CA has limited effect on the improvement of hydrophobicity of the films.

Oxygen resistance performance of modified hemicellulose films

The main functions required for packaging materials include preventing oxidation and deterioration of food. As such, lower oxygen transmission coefficient is a primary concern. A lower oxygen permeability (OP) value represents a better barrier property. The OP values of modified hemicellulose films and some typical packaging materials were summarized in Table 2.

As revealed from Table 2, with the increase of CA content (>20%), the OP value of modified hemicellulose film was greatly reduced from thousands to single digit. The increased barrier property could be explained by the sufficient reaction between

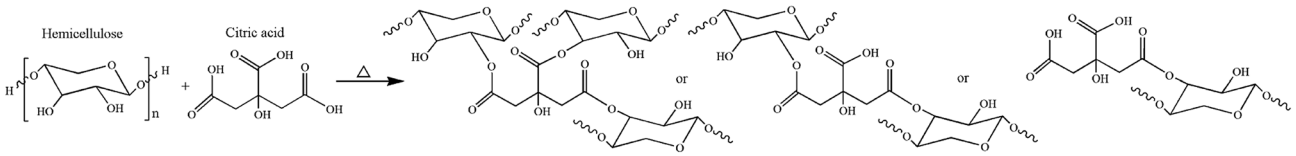

Fig. 2 Possible cross-linking reaction between CA and hemicellulose.

Table 2 Comparison of oxygen permeability of the packaging films in literatures and this work

Sample	Oxygen permeability [(cm^3 μm) (m^2 d kPa)$^{-1}$]
Blank[a]	1053
H_1[a]	1336
H_2[a]	5.4
H_3[a]	7.2
H_4[a]	3.0
H_5[a]	1.8
Spruce galactoglucomannan	6.8 (ref. 31)
Oat spelt arabinoxylan with 40% sorbitol	4.7 (ref. 32)
O-Acetyl-galactoglucomannan with nanofibrillated cellulose	3.2 (ref. 33)
Hydroxypropylated birch xylan	4.7–24 (ref. 34)
Quaternized hemicelluloses with chitosan and montmorillonite	10.95–16.37 (ref. 35)
Low-density polyethylene (LDPE)	7900 (ref. 36)
Poly(lactic acid) (PLA)	160 (ref. 36)
Poly(hydroxyalkanoate) (PHA)	150 (ref. 36)

[a] Test conditions: 23 °C, 50% RH.

carboxyl groups of CA and hydroxyl groups of hemicellulose, which leaded to the formation of cross-linking structure. Crosslinking also reduced the intermolecular gap, thus improving the oxygen barrier performance. Of all the modified films, H_5 film showed the best oxygen barrier performance, with an OP value of 1.8 (cm^3 μm) (m^2 d kPa)$^{-1}$, which was even lower than the other various hemicellulose films in Table 2. All of the OP values of H_2–H_5 films were far lower than those of the typical petroleum-based packaging materials *i.e.* low-density polyethylene (LDPE) and degradable polymer poly(lactic acid) (PLA).[31] This indicated that the modified hemicellulose films possessed great potential in packaging field.

Structural analysis of modified hemicellulose films

The compatibility of the modified hemicellulose films and the interactions between hemicellulose and CA were characterized by FT-IR spectra as shown in Fig. 4. All of the modified poplar hemicellulose films showed obvious C–H stretching vibration peak at 2886 cm^{-1}. On this basis, with the increase of CA content, the absorption peak strength at 1710 cm^{-1}, which represented C=O stretching, increased continuously. It was worth noting that, with the increase of CA concentration, the stretching peak of aliphatic alcohol hydroxyl showed a shift from 3500 cm^{-1} to 3450 cm^{-1}, *i.e.* a redshift. Meantime, the hydroxyl absorption band was significantly enhanced. These results implied that the original intermolecular hydrogen bond was enhanced with increasing CA content. The compatibility of the components in the system was also improved to some extent.[22]

Morphology of the modified hemicellulose films

The microstructures of the hydrophobically modified poplar hemicellulose were characterized by SEM. Representative

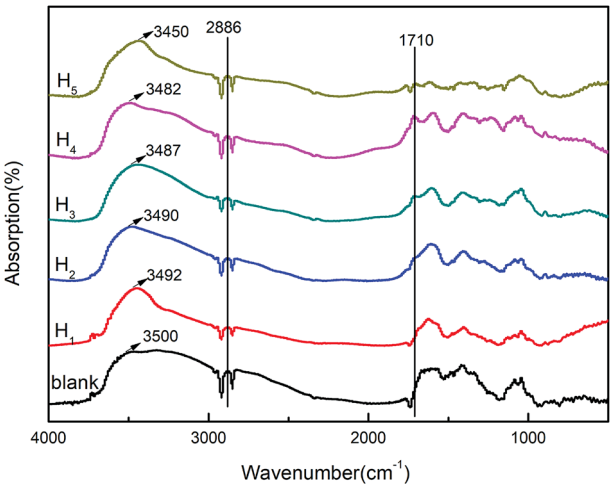

Fig. 4 FT-IR spectra of the hemicellulose films.

images are shown in Fig. 5. The SEM images showed that the surface of poplar hemicellulose film prior to esterification (Fig. 5A) was significantly rougher than that of the esterified films (Fig. 5B–F). The surface roughness decreased first and then increased with the increase of CA. Of the five esterified films, the H_2 film (Fig. 5C) had a flatter, smoother and more compact surface without any gaps, cracks or other defects, implying the better compatibility and dispersion. A possible explanation for these phenomena may be that with the increase of CA content, the esterification reaction and the hydrogen-bond interaction aided hemicellulose in forming a stable cross-linked structure. When the CA content was excessive, the three carboxyl groups of the CA molecule react with hydroxyl groups of hemicellulose selectively. As a result, the overall cross-linking density was reduced, leading to easier slippage between molecular chains, and thus increased surface roughness of the films.

Mechanical properties of modified hemicellulose films

The thickness, tensile strength and elongation at break of modified hemicellulose films were summarized in Table 3, Fig. 6 and 7 for analysis of the effect of CA contents on mechanical properties. Overall, addition of CA increased the thickness of the hemicellulose films. No obvious yield phenomenon was observed in the stretching process of poplar hemicellulose films as revealed from the typical stress–strain curves (Fig. 6). The average tensile strength of the films were found to rise to a peak value and then fell back with the increase in CA content, while the average elongation at break exhibited an opposite trend (Fig. 7). At a CA content of 20% (H_2), the tensile strength reached maximum (about 10.0 MPa), and the elongation at break of the film decreased to minimum (about 5.7%).

A possible mechanism of cross-linking reactions inferred by mechanical performance results is illustrated in Fig. 8. Through the comparison of stress–strain curves for blank, H_1 and H_2, it was deduced that the addition of 10% CA resulted in partial cross-linking of hemicellulose, which affects tensile strength

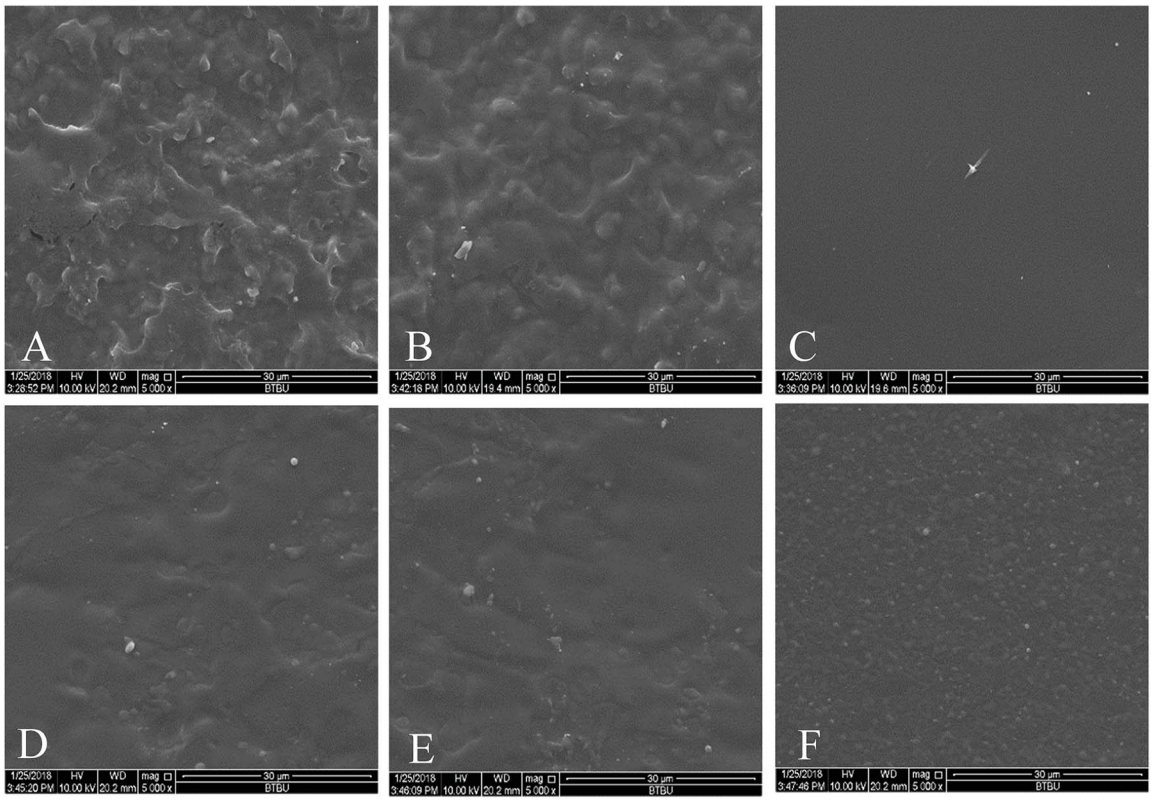

Fig. 5 Representative SEM images of the hemicellulose films. (A) Blank, (B) H_1, (C) H_2, (D) H_3, (E) H_4, (F) H_5.

and elongation at break slightly. In contrast, the films with 20% CA addition showed a higher tensile strength and a lower elongation at break, indicating full cross-linking of hemicellulose and formation of a dense network structure at this level of CA addition. A comparison of stress–strain curves for H_2, H_3, H_4 and H_5 revealed that excessive addition of CA resulted in a significant increase in elongation at break (up to 44.4%) but a notable decrease in tensile strength. This may also originate from the selective reaction of the three carboxyl groups of excessive CA with hydroxyl groups of hemicellulose, which led to increased flexibility of the molecular chain and reduced cross-linking degree of the system. In addition, excessive small CA molecules played a role as plasticizer,[25] which weakens the intermolecular forces and makes the molecular chain more prone to slide, resulting in better film flexibility and poorer mechanical strength. The above discussions are consistent with SEM analysis.

Thermal stability analysis of modified hemicellulose films

The thermal stabilities of modified hemicellulose films were investigated by TGA. As shown in TGA curves of modified films (Fig. 9), the weight loss of all the films were observed at three stages, *i.e.* 60–220 °C (water evaporation), 220–350 °C (main stage of weightlessness) and 350–550 °C (carbonization process).

In the range of 60–220 °C, the weight loss was attributed to the evaporation of weakly physically and strongly chemically bound water for all curves. The weight loss of blank film was the highest among all films in this region, suggesting that the blank film has the largest water absorption. The weight losses of the hydrophobically modified films decreased obviously, which

Table 3 Tensile testing results of the neat and modified hemicellulose films

Sample	Thickness (mm)	Tensile strength (MPa)	Elongation at break (%)
Blank	0.12 ± 0.01	6.3 ± 2.0	8.0 ± 0.9
H_1	0.12 ± 0.01	6.5 ± 0.5	7.6 ± 0.4
H_2	0.13 ± 0.01	10.0 ± 1.1	5.7 ± 1.1
H_3	0.14 ± 0.01	5.8 ± 0.5	11.9 ± 0.8
H_4	0.17 ± 0.01	2.2 ± 0.3	29.9 ± 2.4
H_5	0.20 ± 0.01	2.0 ± 0.2	44.4 ± 2.8

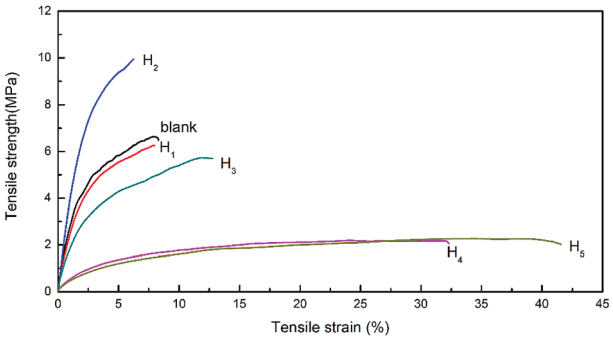

Fig. 6 Typical tensile–strain curves of the hemicellulose films.

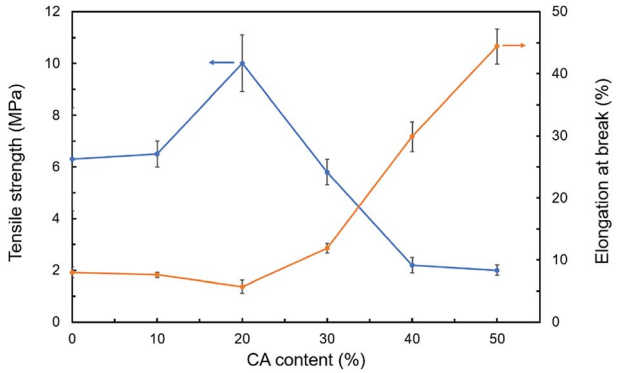

Fig. 7 Mechanical properties of hemicellulose films with different CA contents.

confirmed the hydrophobic modification effect of CA. In a higher temperature range of 220–350 °C, the weight loss was mainly due to the cleavage of C–O bonds and C = O bonds of polymer side chains. In an even higher temperature range, 350–550 °C, the weight loss was attributed to the cleavage of the C–C backbone of the polymer, *i.e.* so-called carbonization.[37] Hydrophobic modification introduced more ester, carboxyl and the like, resulting in less carbon residue, especially for the H_3, H_4 and H_5 films.

The blank film showed a T_{max} (the maximum weight loss temperatures) at 272 °C, whereas T_{max} values for the hydrophobically modified films H_1, H_2, H_3, H_4 and H_5 were found at 284, 304, 304, 308 and 302 °C respectively (Fig. 9B). The T_{max} of the hydrophobically modified film was significantly higher than that of the blank film, indicating that hydrophobic modification of CA could improve the thermal properties of the film. Additionally, when the addition of CA reached 30% or more, two weight loss rate peaks appeared in the region of 220–350 °C due to the decomposition of excess citrate carboxyl groups followed by the cleavage of the polymer side chains. This observation is consistent to the analysis of SEM and mechanical tests.

Conclusions

In summary, citric acid was used as an esterifying agent to modify the hemicellulose films by increasing the surface contact angle to 87.5°, illustrating its superior hydrophobic modification effect. The esterification reaction between CA and hemicellulose constructed cross-linking structure and enhanced the mechanical strength and barrier property in the meantime. When the CA content rose to 20%, the tensile strength of the film was up to 10.0 MPa with the elongation at break of 5.7%. In addition, the hydrophobically modified films exhibited better phase compatibility, preferable thermal stability and lower oxygen permeability. The above results suggested that a facile and green approach *via* chemical cross-linking with CA can be used to produce hemicellulose-based

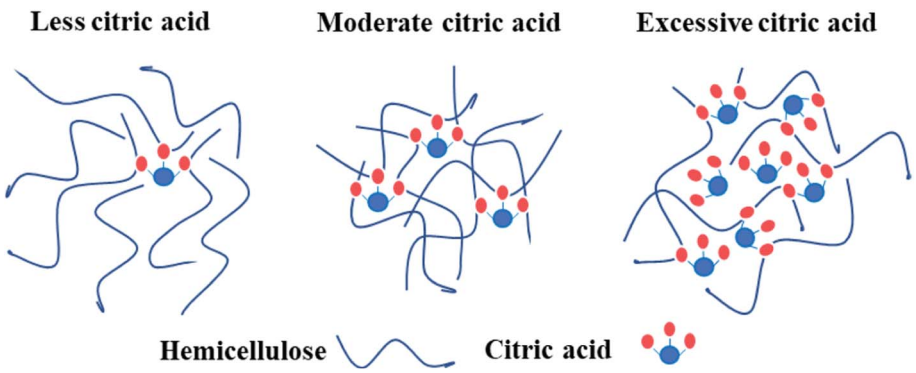

Fig. 8 Possible mechanism of cross-linking reactions between hemicellulose and CA of different contents.

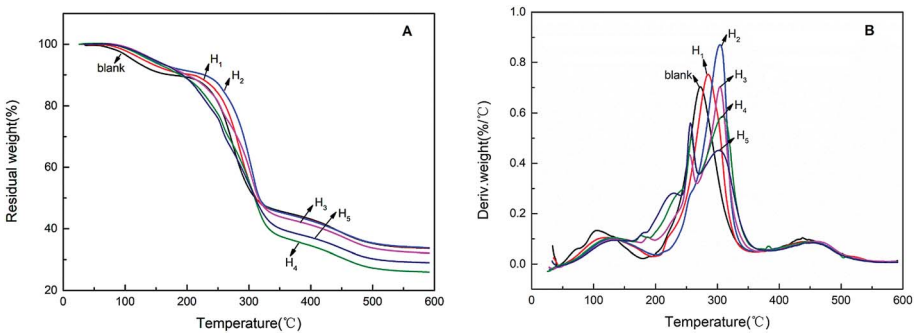

Fig. 9 (A) TGA curves of the hemicellulose films. (B) DTG curves of the hemicellulose films.

films with elevated hydrophobicity. The thus modified hemicellulose films showed great potential in application as alternative food packaging material.

Conflicts of interest

There are no conflicts to declare.

Acknowledgements

Finance support from National Natural Science Foundation of China (Grants No. 31570575, 51473007) and the State Key Laboratory of Solid Lubrication of Lanzhou Institute of Chemical Physics (LSL-1501) is gratefully acknowledged.

References

1 F. Cherubini, *Energy Convers. Manage.*, 2010, **51**, 1412–1421.
2 C.-Z. Chen, M.-F. Li, Y.-Y. Wu and R.-C. Sun, *RSC Adv.*, 2014, **4**, 16944–16950.
3 J. N. Putro, F. E. Soetaredjo, S.-Y. Lin, Y.-H. Ju and S. Ismadji, *RSC Adv.*, 2016, **6**, 46834–46852.
4 N. M. L. Hansen and D. Plackett, *Biomacromolecules*, 2008, **9**, 1493–1505.
5 M. Akkus, E. Bahcegul, N. Ozkan and U. Bakir, *RSC Adv.*, 2014, **4**, 62295–62300.
6 W. Farhat, R. A. Venditti, M. Hubbe, M. Taha, F. Becquart and A. Ayoub, *ChemSusChem*, 2017, **10**, 305–323.
7 F.-Z. Belmokaddem, C. Pinel, P. Huber, M. Petit-Conil and D. Da Silva Perez, *Carbohydr. Res.*, 2011, **346**, 2896–2904.
8 H. Wang, Y. Chen, Y. Wei, A. Zhang and C. Liu, *Carbohydr. Polym.*, 2017, **157**, 1365–1373.
9 A. Ayoub, R. A. Venditti, J. J. Pawlak, H. Sadeghifar and A. Salam, *Ind. Crops Prod.*, 2013, **44**, 306–314.
10 N. G. V. Fundador, Y. Enomoto-Rogers, A. Takemura and T. Iwata, *Carbohydr. Polym.*, 2012, **87**, 170–176.
11 J. L. Ren, R. C. Sun, C. F. Liu, Z. N. Cao and W. Luo, *Carbohydr. Polym.*, 2007, **70**, 406–414.
12 C. Laine, A. Harlin, J. Hartman, S. Hyvärinen, K. Kammiovirta, B. Krogerus, H. Pajari, H. Rautkoski, H. Setälä, J. Sievänen, J. Uotila and M. Vähä-Nissi, *Ind. Crops Prod.*, 2013, **44**, 692–704.
13 M. Alekhina, K. S. Mikkonen, R. Alén, M. Tenkanen and H. Sixta, *Carbohydr. Polym.*, 2014, **100**, 89–96.
14 I. Simkovic, I. Kelnar, I. Uhliarikova, R. Mendichi, A. Mandalika and T. Elder, *Carbohydr. Polym.*, 2014, **110**, 464–471.
15 A. Tressaud, E. Durand, C. Labrugère, A. P. Kharitonov and L. N. Kharitonova, *J. Fluorine Chem.*, 2007, **128**, 378–391.
16 M. Gröndahl, A. Gustafsson and P. Gatenholm, *Macromolecules*, 2006, **39**, 2718–2721.
17 A. Salam, R. A. Venditti, J. J. Pawlak and K. El-Tahlawy, *Carbohydr. Polym.*, 2011, **84**, 1221–1229.
18 W. Zhao, R. W. Nugroho, K. Odelius, U. Edlund, C. Zhao and A. C. Albertsson, *ACS Appl. Mater. Interfaces*, 2015, **7**, 4202–4215.
19 P. Oinonen, D. Areskogh and G. Henriksson, *Carbohydr. Polym.*, 2013, **95**, 690–696.
20 L. M. Zhang, T. Q. Yuan, F. Xu and R. C. Sun, *Ind. Crops Prod.*, 2013, **45**, 52–57.
21 S. Wang, J. Ren, W. Li, R. Sun and S. Liu, *Carbohydr. Polym.*, 2014, **103**, 94–99.
22 Y. Hu, H. Sun, B. Yang, B. Huang and G. Z. Xu, *Acta Polym. Sin.*, 2016, **11**, 1615–1620.
23 J. Hartman, A. Annchristine Albertsson and J. Sjöberg, *Biomacromolecules*, 2006, **7**, 1983.
24 Y. Guan, X. M. Qi, G. G. Chen, F. Peng and R. C. Sun, *Carbohydr. Polym.*, 2016, **153**, 542–548.
25 E. Bahcegul, H. E. Toraman, D. Erdemir, B. Akinalan, N. Ozkan and U. Bakir, *RSC Adv.*, 2014, **4**, 34117–34126.
26 J. Hartman, A. C. Albertsson, M. S. Lindblad and J. Sjöberg, *J. Appl. Polym. Sci.*, 2010, **100**, 2985–2991.
27 Y. Hu, Mphil thesis, Beijing Technology and Business University, 2017.
28 F. Peng, PhD thesis, South China University of Technology, 2010.
29 T. Zhao and L. Jiang, *Colloids Surf., B*, 2018, **161**, 324–330.
30 E. A. Vogler, *Adv. Colloid Interface Sci.*, 1998, **74**, 69–117.
31 K. S. Mikkonen, M. I. Heikkilä, H. Helén, L. Hyvönen and M. Tenkanen, *Carbohydr. Polym.*, 2010, **79**, 1107–1112.
32 K. S. Mikkonen, S. Heikkinen, A. Soovre, M. Peura, R. Serimaa, R. A. Talja, H. Helén, L. Hyvönen and M. Tenkanen, *J. Appl. Polym. Sci.*, 2010, **114**, 457–466.
33 V. Kisonen, K. Prakobna, C. Xu, A. Salminen, K. S. Mikkonen, D. Valtakari, P. Eklund, J. Seppälä, M. Tenkanen and S. Willför, *J. Mater. Sci.*, 2015, **50**, 3189–3199.
34 K. S. Mikkonen, C. Laine, I. Kontro, R. A. Talja, R. Serimaa and M. Tenkanen, *Eur. Polym. J.*, 2015, **66**, 307–318.
35 G. G. Chen, X. M. Qi, Y. Guan, F. Peng, C. L. Yao and R. C. Sun, *ACS Sustainable Chem. Eng.*, 2016, **4**, 1985–1993.
36 C. J. Weber, *Perspect. Biol. Med.*, 2000, **4**, 383–384.
37 L. Yang, H. Y. Zhang, Q. Yang and D. N. Lu, *J. Appl. Polym. Sci.*, 2012, **126**, E245–E251.